ISSN-1996-918X

Pak. J. Anal. Environ. Chem. Vol. 22, No. 1 (2021) 13 – 20

http://doi.org/10.21743/pjaec/2021.06.02

Investigating the Effect of Dwell Time on the Physical Properties of Nano-sized Tin dioxide (SnO_2) Prepared Through a Continuous Microwave Flow Process

Muhammad Akram[1*], Ahmad Sher Awan[2], Asad Gulzar[3] and Muhammad Latif[4]

[1]*Department of Chemistry, Government Degree College, Raiwind (Lahore), Pakistan.*

[2]*Department of Science Education (IER) Quaid-i-Azam Campus, University of the Punjab, Lahore, Pakistan.*

[3]*Department of Chemistry, Division of Science and Technology, University of Education Lahore, Pakistan.*

[4]*Department of Physics, University of Baluchistan, Quetta, Pakistan.*

**Corresponding Author Email: akram786jang@gmail.com*

Received 03 March 2020, Revised 28 October 2020, Accepted 03 November 2020

Abstract

Tin dioxide (SnO_2) is a well-known catalytic material used to catalyze different organic dyes and gas sensors. Similarly, it is also considered a good sensing and optoelectronic material. In this work, SnO_2 has been synthesized using a microwave-assisted continuous flow method. The effect of dwell time was utilized to study its effects on the physical properties of SnO_2. X-ray Diffraction (XRD), Fourier Transform Infrared (FTIR), Transmission Electron Microscopy (TEM) and Bruner Emmit-Teller (BET) techniques were used to characterize the synthesized SnO_2. UV-Visible spectroscopy technique was employed to calculate the energy bandgap, which exhibited a decrease in the energy bandgap from 3.44 to 3.33 eV on increasing the dwell time. XRD results exhibited an increase in the degree of crystallinity from 56 to 63% and a reduction in the particle size from 3.74 to 2.75 nm. Where, BET study revealed a shrinkage in the surface area from 159 to 154 m^2g^{-1}. Photoluminescence (PL) study was conducted to investigate the surface defects. Photocatalytic efficiency of the SnO_2 was probed against the photodegradation of methylene blue dye and this study revealed that SnO_2 is a good photocatalytic material.

Keywords: Retention time, Physical properties, Microwave, Photoluminescence, Energy bandgap, Photodegradation

---

Introduction

Ceramic materials, especially ceramic oxides, are semi-conductor in nature and have widespread applications in many fields like catalysis, magnetic data storage, magnetic resonance imaging and in sensing. It can be used as sensing agents and as sensors towards different gases as good reducing or oxidizing agents in vast areas so as to keep our environment green [1-4]. In this class of oxides, SnO_2 has been identified as the best available material due to its growing and escalating properties such as photocatalytic, electrical, opto-electronic and optical properties [5-7]. In general, these properties are dependent upon their morphology, crystallinity, particle size and especially on their surface area [8-10]. However, the traditional methods to synthesize the SnO_2 nanoparticles are time taking, and some of them produce SnO_2 with particle size well above the microscales, which cannot provide enhanced properties as the nanoparticles in general offer [11-14]. In addition, high temperature or long heating inside the microwave (Mw) may play a potential role in the manipulation of these properties. Rapid

and accelerated preparation of SnO_2 may help in investigating some novel properties.

Many liquid phase methods like sol-gel, hydrothermal, micro-emulsion and sono-chemical have been used to prepare SnO_2 but their long processing time, long post reaction heat treatments, use of toxic solvents and multi-steps make them complex for the synthesis of SnO_2 [11-14]. Mw methods are also now in operation to prepare SnO_2, but the low penetration depth of Mw radiations in the large volume of solvents makes them unpopular [15, 16]. In addition, the synthesis of SnO_2 in the Teflon based autoclaves under high pressure makes them dangerous, as there are some reports of their sudden explosions [17]. To addresses this subject, there is a requirement to reveal some continuous stream systems which may be more fruitful for the fabrication of these important metal oxides [18]. There are few continuous methods which already have been introduced to synthesize various products due to their rapid and proficient mode of heating and to ensure safe and better quality products [19, 20]. The continuous Microwave Flow Synthesis (CMFS) process is relatively a simple, cost effective method. Moreover, it works at ambient temperature and pressure and there is no danger of risks [21].

This paper involves the use of CMFS process, which is a moderately cost-effective, efficient and convenient route to synthesize SnO_2. In this paper, the role of dwell time (heating inside the Mw) on the crystallinity, size, surface area and optical behavior of SnO_2 has been studied. Preliminary results showed a good assembly of visible light active SnO_2 nanoparticles.

Materials and Methods

Chemicals and Reagents

Tin chloride pentahydrate [$SnCl_4.5H_2O$, Merck, Germany], Sodium hydroxide [NaOH, QReC, New Zealand] were introduced to prepare SnO_2. Where methylene blue (Merck, Germany) was used as a reagent for the photodegradation study.

Tin Dioxide Synthesis

0.25 M of $SnCl_4.5H_2O$ in ethanol and 1 M solution of NaOH in ethanol were used to synthesize SnO_2 powder. Both the solutions were then continuously pumped using Longer Pumps Model BT-300-2J (China) separately through Teflon tube (internal diameter 0.2 cm) spirally coiled inside the household Mw (Samsung, Mw 71 B). They were heated inside the Mw for 0, 5 and 10 min operating Mw at 600 W [19] (Fig. 1). The synthesized SnO_2 white precipitates were filtered and washed with doubled distilled H_2O and dried in an oven at 80 ºC for 12 h (equation 1).

$$SnCl_4\ 5\ H_2O + 4\ NaOH \longrightarrow SnO_2 + 4\ NaCl + 7\ H_2O \quad (1)$$

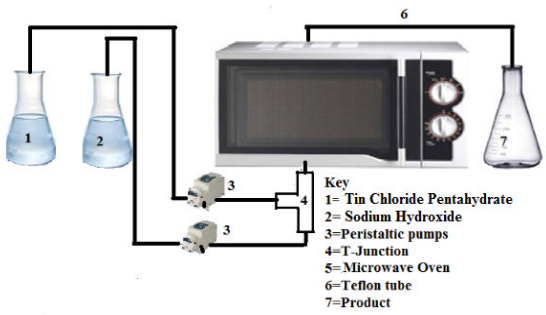

Figure 1. **Schematic representation of CMFS process**

Characterization

To probe the phase purity of the CMFS synthesized SnO_2, Bruker D8, X-Ray diffractometer using Cu-λ radiations (0.15418 nm operating at 40 kV and 40 mA scanning at the rate of .02°/1s at the angle of 2 θ from 20-70°) was used. The degree of crystallinity and particle size was calculated using the standard Scherer equation. Lattice parameters were calculated using a standard unit cell program.

FTIR (Nicolet iS50) was utilized to find out the characteristic functional groups present in the synthesized ceramic oxide. FTIR spectral measurements were made in the range of 4000-400 cm^{-1} averaging at the rate of 32 scans per min. Morphology of the samples was investigated employing TEM (LEO-Libra 120) worked at the speed of 30 kV. A UV-Visible spectrum of the SnO_2 was measured using a spectrophotometer (Lambda 35 Perkin- Elmer) in the range of 300-800 nm to work out the bandgap energy (Eg). To further investigate PL spectra, spectrophotometer (Perkin Elmer, Model LS-50) at an excitation wavelength of 300 nm was used to find out the surface defects that originate in the SnO_2. Similarly, a BET analyzer (Micromeritics Pulse ChemiSorb 2750, USA) was operated between 80 and 90 kPa to determine the surface area measurements.

Photo-catalytic Study of the Samples

Photo-catalytic study of SnO_2 was made against the methylene blue dye (Mb dye). To carry out the photodegradation study, 50 ppm solution was prepared using doubled distilled water. 50 mL solution of SnO_2 was mixed with a sufficient amount of the catalyst and mixed magnetically for 30 min in the dark to homogenize both of the reacting materials. Finally, the UV light (365 nm) was used to irradiate the SnO_2 samples for various intervals of time and each time centrifuged the samples at the rate of 4000 rpm to eliminate the catalyst completely. Then the alteration in the concentration of Mb dye due to the catalytic action of photo-catalysts was measured by recording the absorbance at 637 nm using UV-Visible spectra.

Results and Discussion

The XRD spectrum of SnO_2 prepared on increasing the dwell time inside the Mw from 5 to 10 min has been shown in Fig. 2. All XRD peaks are wide enough, which confirm the formation of nanosized SnO_2 particles with small particle size. The intensity and broadness of the peaks in the case of SnO_2-05-600 (Fig. 2-a) was not as high as it could be observed in the case of SnO_2-10-600 (Fig. 2-b). This increased intensity and sharpness of the XRD peaks thus ensuring that like Mw power, dwell time also have the capability to affect upon the rate of crystallization and size of SnO_2 particles. Results (Table 1) showed that under increased dwell time from 5 to 10 min fixing the Mw power at 600 W and flow rate at fixed position, degree of crystallinity of SnO_2 can be enhanced up to 63% (SnO_2-10-600) from 56% (SnO_2-05-600). Similarly, XRD results indicated reduction in the particle size to 2.74 nm from 3.75 nm on increasing the dwell time.

Table 1. **Textural parameters, degree of crystallinity, particle size and surface area of SnO_2.**

Sample *ID*	a-Axis (A^u)	a-Axis (A^u)	Cell Vol $(A^u)^3$	Crysta-llinity degree (%)	Particle size (nm)	S_{BET} (m^2g^{-1}) Surface area
SnO_2-05-600	4.747	3.188	71.87	56	3.74	159
SnO_2-10-600	4.743	3.182	71.58	63	2.75	154

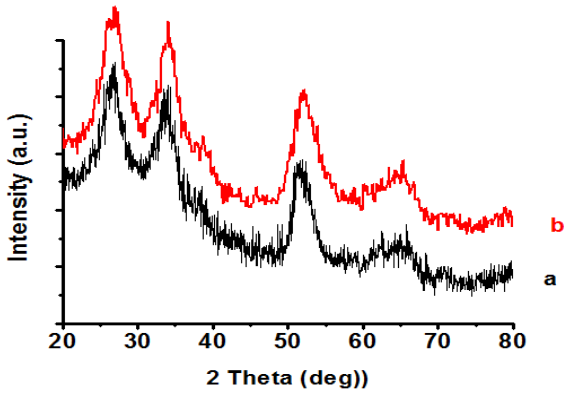

Figure 2. **Influence of dwell time on the XRD patterns of (a) SnO_2-05-600 and (b) SnO_2-10-600**

The enhancement in the crystallinity, particle size and shrinkage in the lattice parameters was calculated using XRD data. Results indicated a reduction in lattice

parameter from a=4.747 ºA and c=3.188 ºA (SnO_2-05-600) to a=4.743 ºA and 3.182 ºA (SnO_2-10-600) (Table 2), which are confirming that dwell time has a significant effect on the textural parameters of SnO_2. Hence, this study reveals that crystallinity, size and surface area of SnO_2 can be alerted on increasing the dwell time of the system on fixed Mw power. Similarly, these results further confirm that the rate of nucleation and growth phenomenon of SnO_2 can also be influenced under the effect of dwell time of Mw and this effect is consistent with the literature [22].

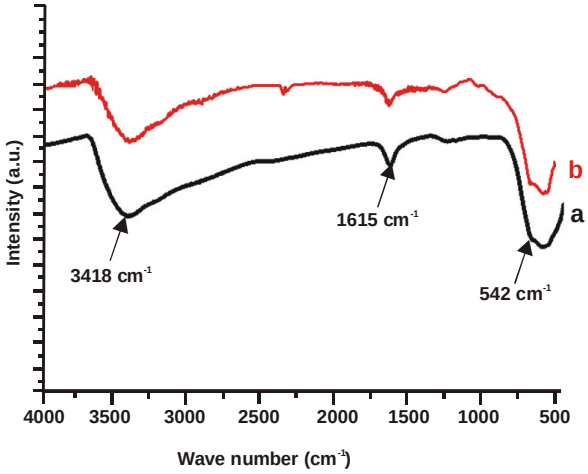

Figure 3. **Influence of dwell time on FTIR spectra of SnO_2 (a) SnO_2-05-600 and (b) SnO_2-10-600**

Figure 3 showed the FTIR spectra for SnO_2, explaining the influence of dwell time on the crystallinity of SnO_2. It contained typical peaks for H_2O (3418 cm^{-1}), a hydroxyl group (1615 cm^{-1}) and a band at 542 cm^{-1} and this was recognized as a bridged O-Sn-O functional group. Boosting up of dwell time to 10 min revealed a reduction of the H_2O and $–OH^-$ peaks and sharpening of the SnO_2 peak, hence further verifying that the augmentation in dwell time at 600 W has the potential to improve the crystallinity of SnO_2. This increase in the crystallinity of the SnO_2 is accredited to the rapid and animated nucleation and growth process, which becomes high in response to dwell time due to rapid collision frequency of ions in the solution and eventually yield is produced with increased crystallinity degree [23].

The morphology of the SnO_2 nanoparticles was observed using TEM micrographs. TEM images of SnO_2-05-600 and SnO_2-10-600 (Fig. 4-a and 4-b) revealed that dwell time does not affect the morphology of the CMFS synthesized SnO_2, however, indicated an increase in the particle size and decrease in the surface area. In addition, TEM images suggested the formation of nanocrystalline SnO_2 nanoparticles.

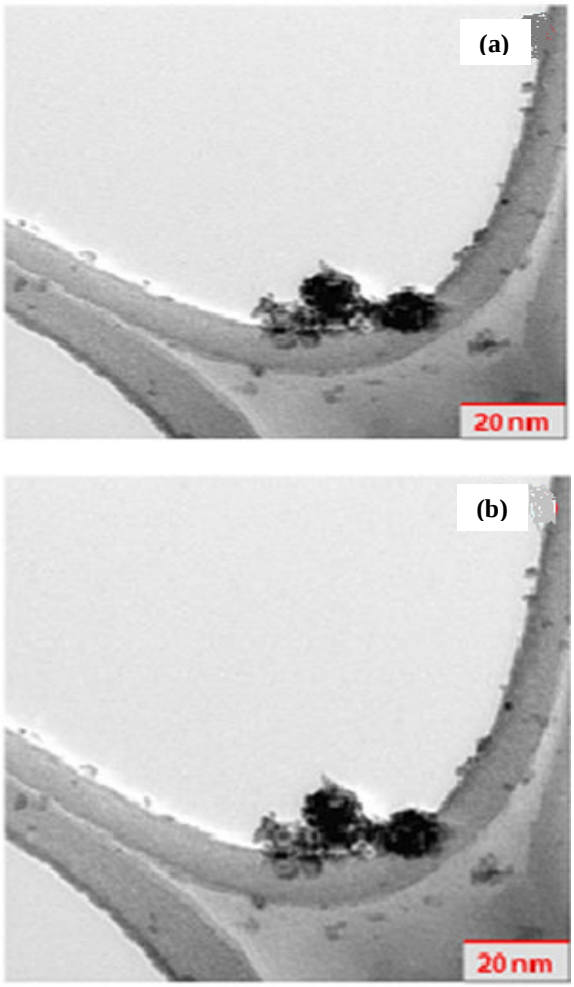

Figure 4. **TEM micrographs of (a) SnO_2-05-600 and (b) SnO_2-10-600**

Furthermore, TEM images showed the formation of agglomerated particles that were not well dispersed and this was because of Vander wall forces that become very strong in the nano region [24]. TEM image of SnO_2-10-600 showed the formation of many coalesced particles with an increase in the particle size and reduced surface area in contrast to SnO_2-05-600 particles and this could be attributed to the high heating rates due to Mw heating and local "hot spots" frequently develop due to high temperature in case of Mw heating. In the case of Mw assisted reactions maximum temperature achieved is controlled by the high boiling of liquids [25]. This phenomenon of "hot spots" raises the temperature of the solution higher than its boiling point. Moreover, the creation of "hot spots" can further reduce the viscosity, which further increases the number of collisions amongst the molecules [26]. This decrease in the viscosity also enhances the tendency of aggregation of SnO_2 nuclei together and thus produces nanoparticles having a small surface area.

The impact of dwell time on the energy bandgap values (E_g) of spherical SnO_2 particles was calculated using UV-VIS spectroscopy (Fig. 5). Association between the absorption coefficients (α) and the photon energy ($h\nu$) for direct allowed transitions was used to calculate the energy band gap of SnO_2 samples (Equation 2) [27]. Here E_g has been used to indicate optical band gap energy, $h\nu$ has been used to show the energy of a photon, α has been applied for the absorption coefficient where A is a proportional constant in this equation.

$$\alpha h\nu = \mathrm{A}(h\nu - \mathrm{Eg})^{n/2} \quad (2)$$

Energy bandgap values for both SnO_2-05-600 and SnO_2-10-600 were found around 3.44 and 3.33 eV. A reduction in the E_g value was observed, which was ascribed to the increased dwell time of Mw from 5 to 10 min (Fig. 5 a and b).

This reduction in E_g values was attributed to the increase in the dwell time. Calculated E_g values (3.44 and 3.33 eV) revealed a redshift compared to the bulk E_g value of SnO_2 (3.6 eV). This redshift in the E_g of SnO_2 could be assigned to lose arrangements and to the high surface area of the particles [28]. Thus, photocatalytic materials like SnO_2 have the capability to harvest more light due to this large surface area. This redshift in the energy bandgap could also be the effect of increased internal stress that goes on increasing due to the reduction in the particle size. Furthermore, reduction of bandgap and energy-level width influence the shift of electron transition from lower to longer wavelength side (valence band to conduction band side) and hence result in the redshift [29].

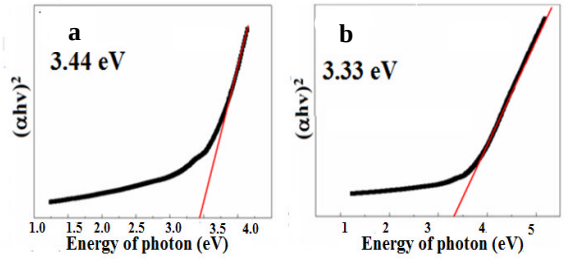

Figure 5. **Energy band gap spectra for (a) SnO_2-05-600 and (b) SnO_2-10-600**

PL technique is periodically applied to resolve the crystalline quality of the nano-sized semiconductors [30]. Fig. 6 showed the PL spectrum of as-prepared SnO_2 nanoparticles. In both cases, a board envelops of emission spectra can be seen around 380 nm due to ethanol. The PL spectra contained a broadband below 400 nm, a sharp band around 430-440 nm and a narrow luminescent band around 480 nm (Fig. 6). The intensity of PL bands revealed a gradual decrease in increasing the dwell time. In common,

products synthesized at ambient conditions were amorphous in nature and have a large number of surface defects and oxygen vacancies therefore, they expose well-built PL signals in the spectra [31].

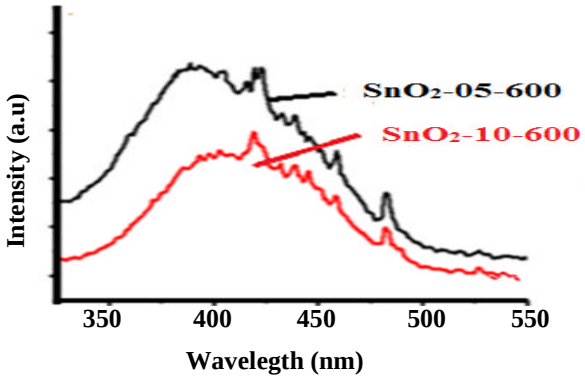

Figure 6. **PL spectra of SnO_2 showing the influence of dwell time**

The PL spectra of SnO_2-05-600 contained a high intensity broadband centered at 435 nm, which was attributed to the existence of surface defects and oxygen vacancies [32]. The reduction in PL intensity in the case of SnO_2-10-600 was assigned to the cutback in the oxygen vacancies and surface defects due to the amplification in the crystallinity of products [30].

Mb dye is the major pollutant of industrial area waters. SnO_2 is a popular catalyst and has the potential to catalyze many organic contaminants under UV light (Hoda-Fujishima effect) [33]. Under ambient conditions and UV-VIS light, toxic organic contaminants that are difficult to decompose can easily be oxidized to H_2O and CO_2 by employing metal-based catalysts and particularly SnO_2 as a catalyst [34-35]. UV light illuminates the surface of the photocatalytic surface and thus produces h^+ hole in the valence band and an e^- in the conduction band. This h^+ can either directly oxidizes the organic contaminant or produce OH^- anion after oxidizing water. Alternatively, e^- in the conduction band has the capability to react with the H_2O molecules present on the surface to produce OH^- anion that further reacts with the dye to produce degradation product or helps in reducing the oxygen absorbed on the surface of the catalyst. SnO_2 was employed to catalyze the Mb dye and the results showed a reduction in the photodegradation of Mb dye on increasing the dwell time from 5 to 10 min (Table 2 and Fig. 7).

Table 2. **Photodegradation of methylene blue against SnO_2.Check plz**

Time (min)	Photodegradation (%) Blank	Photodegradation (%) SnO_2-05-600	Photodegradation (%) SnO_2-10-600
0	50	50	50
30	49.95	39	42
60	49.88	25.5	33.5
90	49.71	12.7	21.41
120	49.63	6.33	13.67
150	49.55	4.09	9.05
180	49.43	2.11	5.15

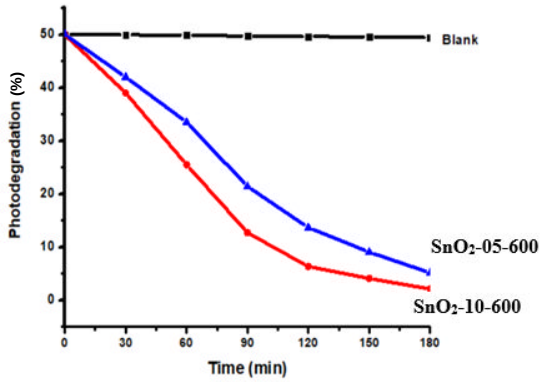

Figure 7. **Influence of SnO_2 catalyst on the Mb dye**

SnO_2-05-600 investigated improved catalytic action in contrast to the SnO_2 sample produced using 10 min dwell time. We believe that this was the effect of the semi-crystalline nature of SnO_2 and its high surface area [36]. However, one thing is more evident from this result that the blank sample synthesized in the absence of Mw heating has negligible photocatalytic efficiency (Fig. 7-Blank).

Conclusion

Phase pure nano-sized SnO_2 was successfully synthesized through a modified Mw method. The influence of dwell time was probed to study its effect upon the physical properties of SnO_2. Results indicated an enhancement in the crystallinity, particle size and reduction in the surface area up to 154 m^2g^{-1}. TEM results showed no detectable transformation in morphology upon increasing the dwell time, however, they displayed an increase in the particle size and this result is in good agreement with XRD result. E_g studies revealed a redshift in the energy bandgap from 3.44 to 3.33 eV, where PL study indicated a decrease in the intensity of peaks due to increased dwell time. Similarly, photocatalytic study of SnO_2 confirmed a rapid photodegradation conversion of around 80-90% of the dye in the first 40 to 60 min. These results confirmed that the CMFS prepared SnO_2 may be a good catalytic material for the photodegradation of various dyes, humidity sensors and gas sensing material, etc., due to its high surface area.

Conflict of Interest

The authors declare that they have no conflict of interest.

References

1. M. Batzill and U. Diebold, *Prog. Surf. Sci*., 79 (2005) 154. https://doi.org/10.1016/j.progsurf.2005.09.002
2. C. J. Martinez, B. Hockey, C. B. Montgomery and S. Semancik, *Langmuir*, 21 (2005) 7944. https://doi.org/10.1021/la050118z
3. M. Akram, R. Hussain, F. K. Butt and M. Latif, *Mater. Res. Express*, 6 (2019) 085041. https://doi.org/10.1088/2053-1591/ab1a0b
4. Z. Li, H. Jiang, N. C. Lai, T. Zhao and Y. C. Lu**,** *Chem. Mater*., 31 (2019) 10196. https://doi.org/10.1021/acs.chemmater.9b03885
5. F. K. Butt, C. Cao, W. S. Khan, Z. Ali, T, Mahmood, R. Ahmed, S. Hussain and G. Nabi, *Mater. Chem. Phys*., 136 (2012) 14. https://doi.org/10.1016/j.matchemphys.2012.04.024
6. F. K. Butt, C. Cao, W. S. Khan, M. Safdar, X. Fu, M. Tahir, F. Idress, Z. Ali, G. Nabi and D. Yu, *Cryst. Eng. Comm.*,15 (2013) 2112. https://doi.org/10.1039/C2CE26728D
7. S. Zaman, J. Xin and F. K. Butt, *Mater. Lett*., 119 (2014) 114. https://doi.org/10.1016/j.matlet.2013.12.064
8. Y. Han, X. Wu, Y. Ma, L. Gong, F. Qu and H. Fan, *Cryst. Eng. Comm.*, 13 (2011) 3510. https://doi.org/10.1039/C1CE05171G
9. F. Li, J. Song, H. Yang, S. Gan, Q. Zhang, D. Han, A. Ivaska and L. Niu, *Nanotechnology*, 20 (2009) 455602. https://doi.org/10.1088/0957-4484/20/45/455602
10. P. Manjula, R. Boppella, and S.V. Manorama, *ACS Appl. Mater. Interf.*, 4 (2012) 6260. https://doi.org/10.1021/am301840s
11. J. Zhang and L. Gao, *J. Solid State Chem*., 177 (2004) 1430. https://doi.org/10.1016/j.jssc.2003.11.024
12. M. Krishna and S. Komarneni, *Ceram. Int*., 35 (2009) 3379. https://doi.org/10.1016/j.ceramint.2009.06.010
13. Y. Wang, J. Y. Lee and T. C. Deivaraj, *J. Mater. Chem*., 14 (2004) 365. http://scholarbank.nus.edu.sg/handle/10635/54380
14. D. N. Srivastava, S. Chappel, O. Palchik and A. Zaban, *Langmuir*, 18 (2002) 4164. https://doi.org/10.1021/la015761+

15. M. Oliveira and A. Franca, *J. Food Eng*., 53 (2002) 359. https://doi.org/10.1016/S0260-8774(01)00176-5
16. M. Oghbaei and O. Mirzaee, *J. Alloy Compd*., 494 (2010) 189. https://dio.org/10.1016/j.jallcom.2010.01.068
17. K. Huang and B. Lu, *Sci. China Technol. Sci.*, 52 (2009) 496. https://link.springer.com/article/10.1007%2Fs11431-008-0286-3
18. G. Jas and A. Kirschning, *Chem-Eur. J*., 9 (2003) 5723. https://doi.org/10.1002/chem.200305212
19. R. Jachuck, D. Selvaraj and R. Varma, *Green Chem*., 8 (2006) 33. https://doi.org/10.1039/B512732G
20. J. Lu, K. Minami, S. Takami, M. Shibata, Y. Kaneko and T. Adschiri, *ACS Appl. Mater. Interf.*, 4 (2011) 354. https://doi.org/10.1021/am2014234
21. M. Akram, A. Z. Shemary, F. K. Butt, Y. F. Goh, W. A. Wan Ibrahim and R. Hussain, *Mater. Lett*., 160 (2015) 149. https://doi.org/10.1016/j.matlet.2015.07.088
22. S. K. Park, K. D. Kim and H.T. Kim, *Colloid. Surf. A*, 197 (2002) 17. https://doi.org/10.1016/S0927-7757(01)00683-5
23. T. Hanrath, and B.A. Korgel, *J. Am. Chem. Soc*., 124 (2002) 1429. https://doi.org/10.1021/ja016788i
24. M. J. Mayo, D. C. Hague and D. J. Chen, *Mater. Sci. Eng. A*, 166 (1993**)** 159. https://doi.org/10.1016/0921-5093(93)90318-9
25. K. Bougrin, A. Loupy and M. Soufiaoui, *J. Photochem. Photobiol. C*, 6 (2005) 167. https://doi.org/10.1016/j.jphotochemrev.2005.07.001
26. R. Al-Gaashani, S. Radiman, N. Tabet, and A. R. Daud, *Mater. Chem. Phys*., 125 (2011) 852. https://doi.org/10.1016/j.matchemphys.2010.09.038
27. P. Praus, O. Kozak, K. Koci, A. Panacek and R. Dvorsky, *J. Colloid Interf. Sci*., 360 (2011) 579. https://doi.org/10.1016/j.jcis.2011.05.004
28. L. Wang, Z. Nie, C. Cao, M. Ji, L. Zhou and X. Feng, *J. Mater. Chem. A*, 3 (2015) 3718. https://doi.org/10.1039/C4TA04182H
29. M. Sabbaghan, A. Anaraki Firooz and V. Jan Ahmadi, *J. Mol. Liq*., 175 (2012) 140. https://doi.org/10.1016/j.molliq.2012.08.019
30. S. Luo, J. Fan, W. Liu, M. Zhang, Z. Song, C. Lin, X. Wu and P. K. Chu, *Nanotechnol*ogy, 17 (2006) 1699. https://doi.org/10.1088/0957-4484/17/6/025
31. J. X. Zhou, M. S. Zhang, J. M. Hong and Z. Yin, *Solid State Commun*., 138 (2006) 246. https://doi.org/10.1016/j.ssc.2006.03.007
32. J. Q. Hu, Y. Bando, Q. L. Liu and D. Golgerg, *Adv. Funct. Mater.*, 13 (2003) 496. https://doi.org/10.1002/adfm.200304327
33. A. Fujishima and K. Honda, *Nature*, 238 (1972) 38. https://doi.org/10.1038/238037a0
34. H. Khan, A. Balouch, K. F. Soomro, H. Shaikh, S. Naz, A. A. Kandhro, M. Q. Samejo and N. N. Memon, *Pak. J. Anal. Environ. Chem*., 20 (2019) 38. http://dx.doi.org/10.21743/pjaec/2019.06.04
35. K. A. Adegoke, M. Iqbal, H. Louis, S. U. Jan, A. Mateen and O. S. Bello, *Pak. J. Anal. Environ. Chem*., 19 (2018) 27. http://dx.doi.org/10.21743/pjaec/2018.06.01
36. E. Y. Kim, D.S. Kim and B. T. Ahn, *Bull. Korean Chem. Soc.*, 30 (2009) 193. https://doi.org/10.5012/bkcs.2009.30.1.193